Safe operation of dual-fuel engines using constrained stochastic control

Carlos Guardiola[1], Benjamín Pla[2], Pau Bares[2] and Alvin Barbier[2]

Abstract

Premixed combustion strategies have the potential to achieve high thermal efficiency and to lower the engine-out emissions such as NO_x. However, the combustion is initiated at several kernels which create high pressure gradients inside the cylinder. Similarly to knock in spark ignition engines, these gradients might be responsible of important pressure oscillations with a harmful potential for the engine. This work aims to analyze the in-cylinder pressure oscillations in a dual-fuel combustion engine and to determine the feedback variables, control actuators, and control approach for a safe engine operation.

Three combustion modes were examined: fully, highly and partially premixed, and three indexes were analyzed to characterize the safe operation of the engine: the maximum pressure rise rate, the ringing intensity and the maximum amplitude of pressure oscillations (MAPO). Results show that operation constraints exclusively based on indicators such as the pressure rise rate are not sufficient for a proper limitation of the in-cylinder pressure oscillations. This paper explores the use of a knock-like controller for maintaining the resonance index magnitude under a predefined limit where the gasoline fraction and the main injection timing were selected as control variables. The proposed strategy shows the ability to maintain the percentage of cycles exceeding the specified limit at a desired threshold at each combustion mode in all the cylinders.

Introduction

Environmental concerns in engine-related air pollution and global warming drove the research community to continuously develop more advanced and efficient technologies. Nevertheless, combustion engine efficiency optimization is a challenging task that comes with its limitations and trade-off, e.g. fuel consumption and pollutant emissions in diesel engines or lack of direct control of the combustion timing and limited operating range in premixed combustion strategies such as homogeneous charge compression ignition (HCCI)[1–4]. Among these limitations, in-cylinder pressure oscillations are a key information to consider in order to provide tools that could be used to develop safe and efficient combustion operation strategies[5].

In spark ignition (SI) engines, the main limiting factor to efficiency improvement is knock. Knock corresponds to the auto-ignition of the end gas, before the flame front reaches all the combustion chamber, which excites heavily the resonant frequencies inside the cylinder and results in thermal efficiency drop and can be responsible of engine damage[6]. Such phenomena might be detected by frequency analysis of the engine block vibration using accelerometers[7,8], or by direct measurement of the cylinder pressure signal[9,10]. According to the recent trend for enhanced control strategies need, in-cylinder pressure sensors appear to be powerful candidates[11]. Nevertheless, such sensors use to lead to added

system complexity and cost which explains why they are traditionally limited to investigation applications[12].

Various indexes can be found to evaluate the knock content[13–15] but the maximum amplitude of pressure oscillations (MAPO) is one of the most common[16,17]. The MAPO is obtained by high-pass filtering the measured in-cylinder pressure trace every cycle and a threshold is traditionally determined empirically from experimental data by the user to avoid engine damage. When combustion conditions lead to unsafe operation where spontaneous auto-ignition of the end gas appears, the MAPO is detected above this limit and the cycle is considered as knocking[18]. Since the spark is responsible of triggering the combustion, knock is essentially controlled by means of spark advance (SA) regulation[19–21]. In the conventional knock control, every cycle the spark angle is advanced by an amount of k_{adv} for engine efficiency improvement, and delayed by a higher amount k_{ret} when a knocking cycle is detected.

[1]Universitat Politècnica de València, Camino de Vera s/n, E-46022 Valencia, Spain
[2]CMT-Motores Térmicos, Universitat Politècnica de València, Camino de Vera s/n, E-46022 Valencia, Spain

Corresponding author:
Alvin Barbier, CMT-Motores Térmicos, Universitat Politècnica de València, Camino de Vera s/n, E-46022 Valencia, Spain.
Email: albar9@mot.upv.es

Detailed reviews about knock phenomena can be found in Zhen et al.[13] and Wang et al.[22].

In compression ignited (CI) engines, the safe operation of conventional diesel combustion (CDC) is commonly associated to its maximum pressure rise rate (MPRR) and engine noise level which is affected by the pressure oscillations caused by the combustion[23,24]. Multiple injection strategies aim to reduce the amount of fuel burned in premixed conditions with a short pilot injection combustion. This lowers the ignition delay of the main injection and hence act on the pressure rise rate and the oscillations intensity[25,26].

New low temperature combustion (LTC) modes such as HCCI or reactivity controlled compression ignition (RCCI) aim to emit low NO_x and low soot concentration thanks to longer ignition delays[27–29]. They are nevertheless limited by their MPRR levels due to the rapid auto-ignition of the mixture[30–32] and use to exhibit high resonance excitation[33]. Similar to knock in SI engines, the resulting pressure waves represent a source of potential damage for the engine and must be limited and controlled. The ringing intensity (RI) proposed by J.A. Eng[34] to evaluate the pressure waves is a commonly adopted index for this kind of combustion where a criterion of 5 MW/m^2 is often considered to differentiate knocking from non-knocking cycles[35,36].

Shahlari et al.[37], Wissink et al.[38] and Dernotte et al.[39] studied the pressure oscillations in various combustion modes using different indexes such as the MPRR, RI and characterizing the combustion noise generated by the pressure waves using power spectral density (PSD) analysis. It was highlighted that the magnitude of the three indexes are not always correlated and that the levels of MPRR and RI are highly dependent on the processing of the cylinder pressure signal. The raw data is subject to noise amplification when calculating its gradient and this might bias the detection of ringing event. However, filtering may remove some information and provide noticeably different values of MPRR and RI. Consequently, it is important to clearly define the filter characteristics along with the results.

In dual-fuel engine applications, Selim[40] considered the MPRR as an index to study knock. The engine used pure methane (CH_4), compressed natural gas (CNG) and liquefied petroleum gas (LPG) as the main fuels, and diesel as the ignition source. He found that advancing the diesel injection resulted in higher ignition delays and thus increased the maximum cylinder pressure and MPRR levels. Kirsten et al.[41] proposed a knock event detection which separates the ringing oscillations due to the premixed combustion and the knocking combustion of the end-gas in a natural gas/diesel engine. The detection method calculates a factor using the information from each phase and compares it to a threshold. The knock threshold was calibrated by analyzing cylinder pressure traces and evaluating if the cycles were in non-knocking or knocking conditions. They compared the data from in-cylinder pressure sensor and conventional knock sensor at various operating conditions, e.g. lambda and intake temperature, showing a good agreement in the

detection of the knocking cycles. Lounici et al.[42] also studied knock in natural gas/diesel engines. In this case the MAPO was used and they found that the brake thermal efficiency and the emissions were worsened under knocking conditions. In addition, as the knock intensity was increased a higher cyclic variability of the index was noticed. The MAPO was also used by Chen et al.[43] to study the cyclic knock variability in a methane/n-heptane CI combustion engine varying the timing of the n-heptane injection. In this case, higher levels of MAPO were obtained at higher premixed conditions. They optically observed the multipoint auto ignition process of the combustion and stated that the pressure oscillations were induced by local fast burning rate.

While it is common to find studies about the definition of knock and combustion noise indexes in premixed combustion engines and how the control variables would affect them (some additional examples might be found in the literature[44–46]), few of them were dedicated to implement the strategies in a real-time control application. In particular, most of the works that proposed such kind of controller used the MPRR as the limitation value[47–50] but did not assess the pressure oscillations. Mashkournia et al.[51] implemented a controller in an HCCI engine where the knock was detected by a discrete wavelet transform of the pressure oscillations. A threshold was experimentally determined and the controller kept the knock index close to the desired value by regulating the fuel octane number of the mixture (dual injectors of n-heptane and iso-octane).

This work aims to study the combustion pressure oscillations in a dual-fuel engine and to evaluate a control strategy for ensuring a safe operation of the engine. In particular, three operating conditions are investigated: fully, highly and partially premixed combustion. The respective pressure rise rate, ringing intensity and amplitude of pressure oscillations levels are analyzed and it is shown that: each combustion mode results in distinct resonance excitation, and indexes based on low-pass filtered signals such as the MPRR may lead to an underestimation of the pressure oscillations magnitude. A combustion sensitivity study is then performed to investigate the influence of the control variables on the resonance and based on these conclusions, a knock-like controller using the gasoline fraction and the diesel injection timing to control the MAPO is proposed and validated in the different combustion strategies showing the ability to control the number of cycles exceeding the resonance index limit in all the cylinders. Here, individual in-cylinder pressure sensors were used as feedback information about the combustion to obtain the limitation factors. Although these sensors are not widely found in on-road applications, the designed control strategy was yet considered relevant because the index obtained by this method might be substituted by another one coming from competitive cylinder pressure measurement techniques or non-intrusive estimation approach[52–55] and still be applicable, as long as a sensitivity to the chosen control inputs exists.

The article is structured as follows: first, a brief description of the experimental facilities and the acquisition and signal

processing tools used in this study is presented. Next, the investigated combustion modes are introduced and followed by an analysis of the resonance detection methods where it is shown that existing indexes may lead to different conclusions. According to the previous analysis, a control strategy is proposed based on combustion sensitivity results. The controller is then validated at each combustion mode and finally, the last section highlights the contribution of this paper and summarizes the results.

Experimental facilities

The engine used in this study was a six cylinder heavy-duty diesel engine, which specifications can be found in Table 1, modified to run in dual-fuel combustion by adding a port fuel injector (PFI) at each cylinder.

Table 1. Engine specifications

Bore x Stroke	110 mm x 135 mm
Connecting-rod length	212.5 mm
Compression ratio	12.2:1
Number of cylinders	6
Total displacement	7700 cm^3

In this work the high reactivity fuel was diesel and it was direct injected (m_{di}) at a rail pressure P_{rail} controlled by the commercial engine control unit (ECU). The low reactivity fuel, i.e. gasoline, was port fuel injected (m_{pfi}) at a constant injection pressure of 7 bar. The gasoline fraction (GF) corresponds to the ratio of gasoline to the total fuel injected:

$$GF = \frac{m_{pfi}}{m_{pfi} + m_{di}} \tag{1}$$

The control of the injection settings at each cylinder, i.e. duration of injection (DOI) and start of injection (SOI), was carried out using dedicated devices connected to an embedded Field Programmable Gate Array (FPGA) chassis from National Instruments (NI 9155). A NI 9752 module was used for cam and crank angle synchronization and the injectors pulses were generated by two NI 9751 and two NI 9758 modules for the direct and the port fuel injection, respectively.

The engine is equipped with a variable geometry turbine (VGT) for varying the boost pressure controlled by the ECU, both low pressure (LP) and high pressure (HP) exhaust gases recirculation (EGR) valves controlled by CAN (PXI-8512) and a back pressure (BP) valve at the exhaust to provide the desired air dilution controlled by an analog signal generated by the real-time controller (PXIe-8135). The EGR amount was calculated using the CO_2 balance at the intake and the exhaust using an Horiba Mexa-One gas analyzer.

An in-cylinder pressure sensor from Kistler, type 6125C, was mounted in each cylinder (P_{cyl}) and the intake pressure (P_{int}) was measured by a Kistler 4045A10 sensor. Both signals were monitored with a sampling frequency function of the engine speed using a research encoder set with a
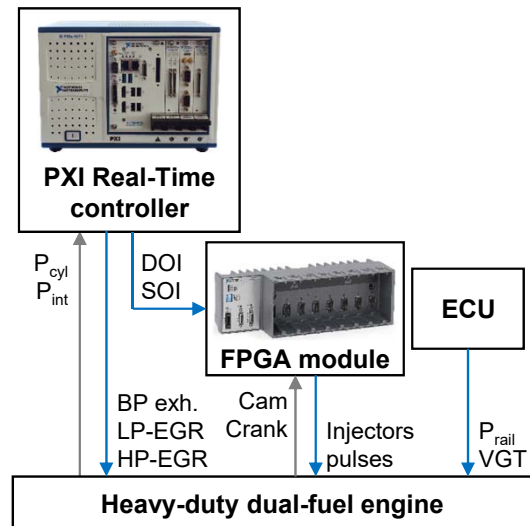

Figure 1. Experimental facilities layout: control actions (blue) and data acquisition (grey)

resolution of 0.2 crank angle degree (CAD) per sample. The acquisition of the different signals was handled by a 16 analog channels acquisition card (PXIe-6358) connected to the real-time controller (PXIe-8135) from National Instruments which was in charge of processing and saving the data. A scheme of the control and acquisition layout is shown in Figure 1.

The in-cylinder pressure *pegging*[56] was done using the intake manifold pressure near the intake bottom dead center (BDC) and the signal was filtered at 2.5 kHz. The cutoff frequency was chosen according to the resonant frequency calculation for the first circumferential mode in a cylindrical combustion chamber[57] where the axial modes are neglected as in (2), where $B_{1,0}$ is the Bessel constant, c the local speed of sound and D the engine bore. Using dual-fuel combustion data from low up to full load from the studied engine it was found that the first mode frequency was ranging from 3 to 5 kHz in the -20 to 40 CAD after top dead center (aTDC) window. Hence, 2.5 kHz was chosen to separate the combustion content (i.e. low-pass filtered signal, p_{lp}) from the pressure oscillations (i.e. high-pass filtered signal, p_{hp}). The heat release calculation and the combustion metrics such as the indicated mean effective pressure (IMEP) and the crank angle where 50% of the energy has been released (CA50) were obtained from the low-pass filtered signal.

$$f_{1,0} = B_{1,0} \frac{c}{\pi D} \tag{2}$$

Dual-fuel combustion strategy

Dual-fuel combustion offers additional degrees of freedom to control the combustion reactions and might therefore be found in various injection strategies[58,59]: at low loads, the gasoline fraction is used to modify the reactivity of the mixture, while at high loads, the diesel injection triggers the combustion in a strategy characterized by the stratification of the late diesel injection and the fuel that has been mixed previously.

In this work, three typical combustion concepts were evaluated, namely: fully premixed, highly premixed and partially premixed. Each combustion mode is commonly associated to a specific area of the engine operating map as illustrated in Figure 2:

- At low load, the highly premixed condition is used to ensure enough mixture stratification to ignite at the right moment and thus provide a well phased combustion.
- By increasing the load, more energy is available and the diesel injections can be advanced to reach fully premixed conditions. This results in high mixing times and therefore ensures low NO_x and soot emissions.
- Finally, at high loads the rapid auto-ignition of the mixture becomes critical and only partially premixed combustion can be safely achieved. To this aim, a single diesel injection is moved in the vicinity of the top dead center to reduce the amount of premixed charge. In these conditions the combustion might show some diffusive-like behavior, which penalizes the total NO_x emissions but extends the operating range of the dual-fuel combustion.
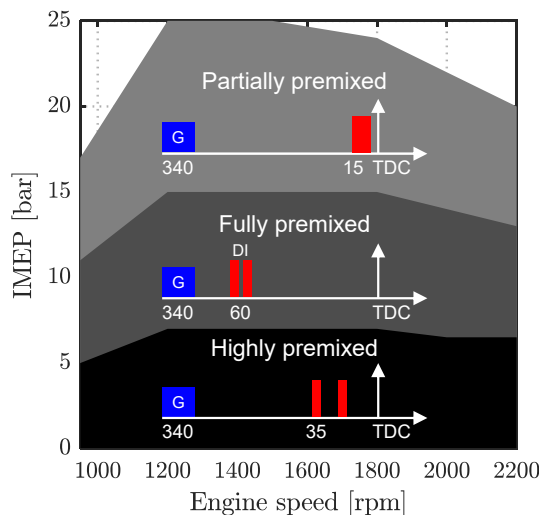

Figure 2. Injection strategy for each combustion mode in the engine operating map. In blue is shown the gasoline injection (G) and in red are illustrated the diesel injections (DI). The numbers under the injections representation stand for the injection timings indicated in °bTDC

For illustration and comparison purposes a medium-low load point was selected where all the combustion modes can be tested by applying the appropriate control inputs, namely EGR, gasoline fraction, and diesel injection timings. Table 2 collects the information from the main control inputs required for performing such modes and the respective in-cylinder pressure and heat release rate (HRR) evolution are shown in Figure 3. This figure shows the cycle-to-cycle signal from 500 consecutive cycles at steady-state operation in grey, and an individual selected cycle is highlighted in black.

Resonance detection methods

In Figure 4 are illustrated the in-cylinder pressure oscillations from the experimental conditions shown in Figure 3. The rapid combustion of the premixed charge heavily excites the in-cylinder pressure resonance leading to important pressure oscillations which might persist till the end of the piston stroke. It can be observed that the oscillations of the in-cylinder pressure signal are influenced by the combustion events: note that in fully and highly premixed combustion conditions (OP 1 and OP 2) the pressure oscillations are lower in magnitude compared to the partially premixed case (OP 3). In the latter case, a premixed mixture with low reactivity is suddenly burned by the first reactions of a late diesel injection combustion and significant inhomogeneities might lead to high pressure oscillations at some conditions. Substantial combustion pressure oscillations might be a source of thermal efficiency loss and possible damage for the engine and therefore need to be tracked.

Among the various existing indexes to characterize the harmful potential of the combustion operation, three of them were mentioned in the introduction section: the maximum pressure rise rate (MPRR), the ringing intensity (RI) and the maximum amplitude of pressure oscillations (MAPO). While the first one characterizes how fast the combustion pressure evolves, the last two aim to describe the pressure oscillations generated by the combustion. Due to the extensive use of the MPRR in the literature as a combustion operation limitation, this index is analyzed along with the RI and the MAPO as well.
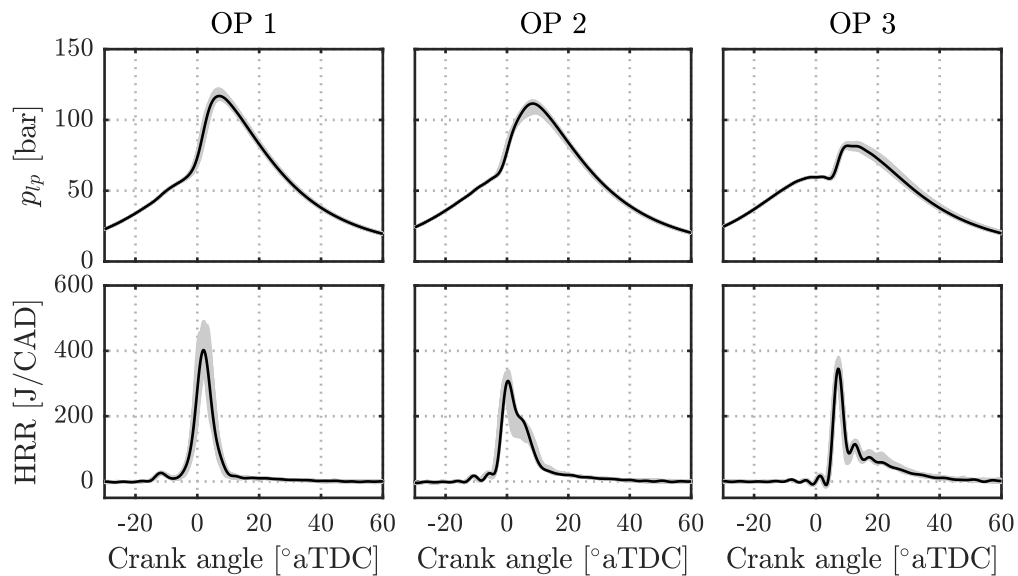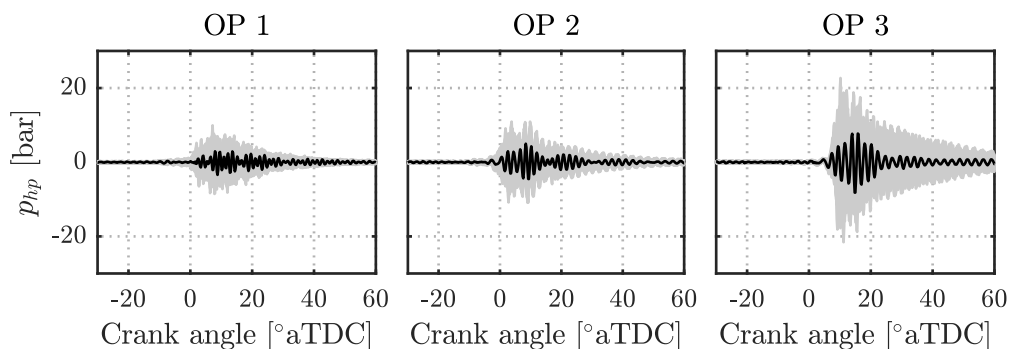
The MPRR, expressed in bar/CAD, is obtained with the maximum value of the first derivative of the filtered pressure signal p_{lp}. This index has been widely used as a mechanical constraint to limit the combustion operation due to its easy calculation and implementation in real-time applications. Nevertheless, being based on the low-pass filtered pressure trace, this index alone fails to capture the combustion pressure oscillations as it was highlighted by Wissink et al.[38]. Assuming that high pressure rise rates stimulate pressure oscillations in the combustion chamber, the ringing intensity, expressed in MW/m^2, was proposed by Eng[34] to estimate the intensity of the pressure waves with the following correlation:

$$RI \approx \frac{1}{2\gamma} \frac{\left(\beta \left(\frac{dP}{dt}\right)_{max}\right)^2}{P_{max}} \sqrt{\gamma R T_{max}} \qquad (3)$$

where $(dP/dt)_{max}$, P_{max} and T_{max} are the maximum pressure rise rate (kPa/ms), cylinder pressure (kPa) and temperature (K), respectively. Note that $(dP/dt)_{max}$ is the time-based equivalent of the crank-based MPRR mentioned earlier. The adjustable term β aims to relate the pressure oscillations amplitude to the pressure rise rate and is often considered to be 0.05, while γ is the heat capacity ratio and R the gas constant. This method was found to be more robust but sensitive to the calibration of β and, as it was pointed out by Dernotte et al.[39], this correlation was originally designed to be implemented in zero- and one-dimensional engine models which do not account for any information of

Table 2. Operating conditions for each of the investigated combustion modes

Parameter	Unit	Fully premixed	Highly premixed	Partially premixed
Operating point	(OP)	1	2	3
Engine speed	[rpm]	1800	1800	1800
IMEP	[bar]	12.5	12.4	11.2
CA50	[°aTDC]	2.5	3	12
P_{int}	[bar]	2.05	2.15	2.15
T_{int}	[°C]	63	67	60
EGR	[%]	44	43	33
GF	[%]	63	62	62
SOI_{pilot}	[°bTDC]	60	34	none
SOI_{main}	[°bTDC]	46	19	10

Figure 3. Pressure signals (top plots) and heat release rate (bottom plots) for different dual-fuel combustion strategies (grey: series of 500 consecutive cycles, black: individual selected cycle)

Figure 4. In-cylinder pressure oscillations for different dual-fuel combustion strategies (grey: series of 500 consecutive cycles, black: individual selected cycle)

the pressure waves. The ringing intensity shares therefore similar limitation with the MPRR. Lastly, the MAPO directly measures the maximum absolute value of the pressure oscillations amplitude through the p_{hp} signal and is expressed in bar. Although this index addresses explicitly the measured pressure waves, it is implicitly sensitive to the pressure trace measurement aspect, e.g. pressure transducer location. Finally, it must be noted that the three indexes share the common attributes of being sensitive to the filter definition and of having a threshold definition, to separate knocking from non-knocking cycles, which is function of the application, the engine and is traditionally empirically set.

Figure 5 shows the corresponding distribution of the MPRR, the RI and the MAPO for all the operating conditions listed in Table 2 with box and whiskers plots. Reducing the premixing time of the mixture allows to decrease the MPRR and RI levels, but it can be observed that in contrast the MAPO level increases, showing that indexes such as the MPRR alone lack of resonance content estimation ability. The similar RI magnitude noticed in OP 2 and 3, although the MPRR was reduced, is likely to be justified by the maximum pressure and temperature compensation, see (3). Furthermore, it can be seen that the measured ringing intensity levels exceed the traditional limit of 5 MW/m^2 although the MPRR is below the considered safety margin of 15 bar/CAD in this engine, showing the calibration and engine dependency of the resonance indexes. Also, it must be noticed that the variability of the MPRR and RI decreases as it approaches partially premixed conditions but the expected oscillations have, on the opposite, an important cycle-to-cycle variability, i.e. from 2.5 to more than 20 bar of MAPO showing the stochastic nature of the resonance excitation. Overall, this figure shows that an opposite trend may be detected when addressing the pressure oscillations with a direct measurement such as MAPO compared to an indirect one like the MPRR. Consequently, high resonance excitation might be identified although safer operation would be supposed by the pressure rise rate reading alone. For this reason, the MAPO was therefore chosen as the resonance index to analyze in the following sections.
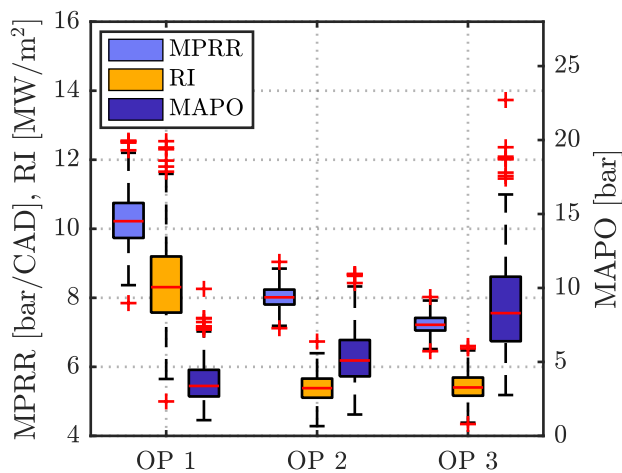

Figure 5. Comparison of MPRR, RI and MAPO levels in the three evaluated combustion modes

Highly premixed conditions are commonly associated with an important cyclic combustion evolution variability due to the inhomogeneities at the combustion ignition (kinetically controlled combustion)[60]. Additionally, multicylinder engines might present uneven fuel distribution from the PFI system, direct injectors ageing, or EGR dispersion between cylinders when using high pressure EGR conditions[61,62]. Henceforth, the resonance intensity of a given operating condition can be understood as a stochastic phenomena, in the same way than knock is understood in spark ignited engines.

In Figure 6, the MAPO probability density function (PDF) at each cylinder in the dual-fuel engine at each combustion mode is illustrated. The resonance intensity observed at each cylinder shows that: first, each cylinder should be controlled individually, and second, that the resonance intensity is random in nature, and hence, the control should be addressed from this perspective. In the present study, it can also be noticed that cylinder 1 exhibits a distinct amplitude distribution compared to the general trend in the other cylinders. This was attributed to the pressure sensor location in the cylinder where the pressure oscillations may be sensed differently[63].

Indeed, as shown in Figure 7, the tested engine was equipped with five pressure sensors positioned at the same location for cylinder 2 to 6, while cylinder 1 had a pressure sensor in a different location for engine geometry reasons. The transducer position has an important role in the measurement of the high frequency component of the combustion pressure. The majority of the resonance content released by the combustion was found to be characterized by the first two circumferential modes[38,39] and their measurement depends therefore on the combustion chamber geometry and the pressure sensor location. As an example, it is not recommended to use centrally mounted transducers when investigating knock-like phenomena[12] because such configuration would mainly detect the first radial mode, and identical pressure sensor properties and mounting in all the cylinders is therefore advised. This can be further understood in Figure 8 where the first two circumferential (m) and the first radial modes (n) in a cylindrical chamber are illustrated[57], from left to right respectively. In this figure the lines represent the nodes where the pressure is constant, hence, if the pressure transducer is located in one of these nodal lines the corresponding resonant mode detection becomes challenging[64].

Resonance excitation and control in dual-fuel engines

In order to ensure a safe operation of the engine it is necessary to find which control variables drive the knock index (MAPO in this case). In Figure 4 it was shown that the combustion conditions, e.g. rate of energy released, start of combustion, mixture stratification, affect the pressure oscillations amplitude. Accordingly, each combustion mode is expected to exhibit a different sensitivity to the control inputs depending on the conditions. The combustion might be controlled by the injection strategy such as the gasoline fraction (GF) or the start of injection (SOI) of the direct injected diesel, as well as by the air-path (EGR, intake temperature, etc). Nevertheless, in order to ensure a fast and safe control of the engine operation, the injection strategy only was considered here for its ability to modify the combustion within a cycle resolution. It was therefore decided to investigate the combustion sensitivity to a change in the gasoline fraction and the start of the main diesel injection for the three operating points discussed in the
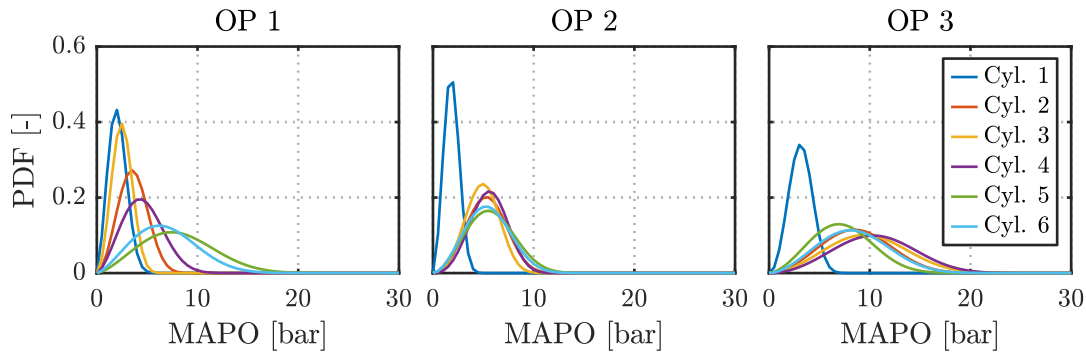
Figure 6. Individual cylinder MAPO probability distribution in all the combustion modes
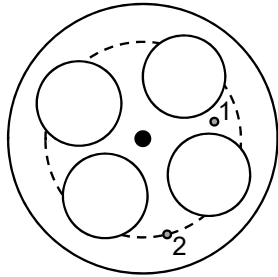

Figure 7. Scheme of the in-cylinder pressure sensors location. Location 1: cylinder 1, location 2: cylinder 2 to 6
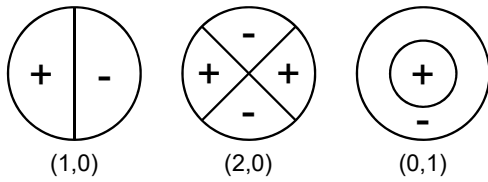

Figure 8. Resonant modes in a cylindrical chamber where circumferential (m) and radial (n) modes are indicated in the form (m, n)

previous section and the results are shown in Figure 9. For the sake of clarity, note that this figure shows the probability density function from only one cylinder.

In this figure it was found that the resonance was mainly driven by the gasoline fraction in fully premixed conditions, where higher gasoline rates reduced the average levels, while the injection timing effect was less clear. This was to be expected due to the kinetically controlled combustion in these conditions. Indeed, due to the early injection timings and high mixing times in this combustion mode, a slight change in the injection timing is believed to not affect drastically the combustion evolution. On the other hand, the gasoline fraction acts on the in-cylinder global reactivity which results in a modification of the combustion development[65] where the resonance might be excited in a higher amount, e.g. the combustion energy is released at once closer to the top dead center by advancing the combustion. Once the diesel injection timing is getting closer to the top dead center, the effect of this control variable becomes more relevant in the knock index distribution as it is shown

in the partially premixed case (OP 3) where advanced timings resulted in higher resonance amount. This is due to the mixture stratification modification resulting from the change in SOI. By approaching the TDC vicinity, the mixture becomes less homogeneous and richer local equivalence ratios appear which enhance the combustion reactions. Contrary to the fully premixed case, here the gasoline fraction is seen to have no clear effect on the MAPO distribution where the first reactions of the diesel injection with the premixed gasoline are found to excite the in-cylinder pressure resonance in a similar way at these levels of mixture reactivity. For its part, the highly premixed condition represents an in-between case where both gasoline fraction and injection timing have some control authority depending on the conditions and where a transition in the combustion regime might be observed[66].

The proposed control strategy to ensure a safe operation of the engine by controlling the resonance intensity in the combustion chamber is based on its stochastic nature. The probability distributions such as shown previously in Figure 9 can be used to set an index threshold not to be exceeded with a predefined probability. The controller should then always ensure that, independently of the combustion mode operated, the probability of having a cycle above the threshold will be maintained at a certain value. This threshold is defined for engine safety and durability and can be shared at each cylinder, considering that the pressure oscillations are equally measured and processed in all the cylinders, e.g. pressure sensor location.

A commonly used technique for such purpose is the conventional knock control, which continuously modifies a given input (u) at every engine cycle k by a certain amount k_{adv} till an event above the knock index (KI) threshold is detected[67] (note that although the observed pressure oscillations phenomena differs from traditional knock in SI engines, here the word *knock* is sometimes used instead of *resonance* when referring to the index to facilitate the description). Once such event appears, the input is modified in the opposite direction by a larger amount k_{ret}:

$$u_k = \begin{cases} u_{k-1} - k_{ret}, & \text{if } KI > KI_{lim} \\ u_{k-1} + k_{adv}, & \text{otherwise} \end{cases} \qquad (4)$$
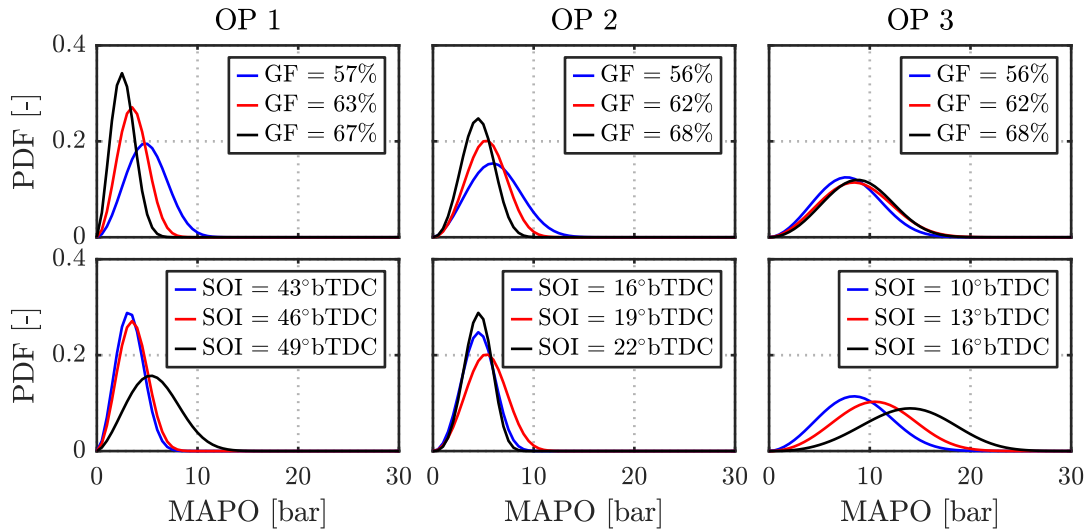
Figure 9. Maximum amplitude of pressure oscillations sensitivity to control inputs in all the dual-fuel combustion modes: gasoline fraction (top plots) and diesel injection timing (bottom plots)

where k_{adv} and k_{ret} calibration defines how fast the controller approaches the operation limit (KI_{lim}) and how the input is modified when an event is detected.

Under stable operation, it is supposed that on average both increments should cancel each other. Considering that k_{ret} (i.e. knock event) occurs with a probability p, these two parameters can therefore be linked by the following relation[68]:

$$k_{adv} = \frac{p}{1-p} k_{ret} \qquad (5)$$

Consequently, if the probability p is considered as a design parameter, either one of k_{adv} or k_{ret} should be defined to fully characterize the controller. By adjusting these parameters, a trade-off can be found between fast response to knocking events and high control actions dispersion[19].

Finally, note that this work investigates the use of MAPO which is obtained from the in-cylinder pressure measurement but one could evaluate the pressure oscillations intensity using another index or technique, e.g. conventional knock sensor on the engine structure, and yet implement the proposed strategy, as long as a sensitivity to the selected control inputs exists.

Results and discussion

The gasoline fraction and the injection timing were evaluated as the control variables in a knock-like controller according to the parameters listed in Table 3 to maintain the probability of cycles with a MAPO above a specified threshold in the three considered combustion modes. Note that here, the percentage of events p and k_{ret} were selected to characterize the proposed controller and k_{adv} was therefore calculated on-line using (5). A scheme of the combustion resonance controller used to obtain the following results is illustrated in Figure 10 where u_k corresponds to either GF or diesel

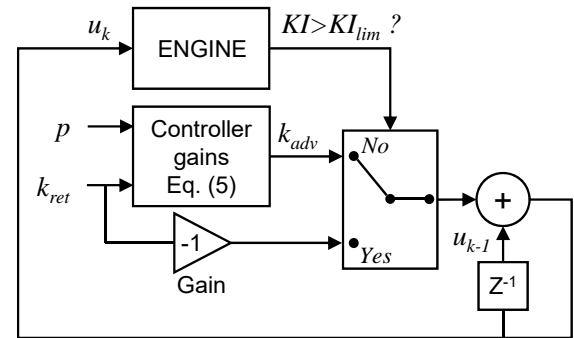main SOI, and KI is the chosen index, in this case: MAPO.

Figure 10. Knock-like controller architecture applied to the dual-fuel engine where u_k corresponds to either GF or SOI, and KI can be MAPO or another designed index

A summary of the results can be found in Table 3 where the obtained probability of exceeding cycles is named p_{ki}. Note that due to the different levels obtained in cylinder 1 (see Figure 6), it was decided to not include this cylinder in the controller validation. Therefore, in the table are indicated the median, minimum and maximum probability from cylinders 2 to 6. When a control variable had no authority on the resonance intensity, the percentage of events could not be controlled, leading to undesired values as discussed in the following conclusions.

Here the results were obtained considering that the combustion sensitivity sign is known, e.g. the gasoline fraction should be increased in fully premixed conditions to decrease the resonance levels, and each control variable was tested independently. Therefore, a control architecture where both control inputs would be actuated and where an automatic transition from one mode to the other would be applied was not evaluated in this work.

Table 3. Operating conditions and results from the tests performed to evaluate the knock-like controller at each combustion mode

		OP 1		OP 2		OP 3	
	Test	1A	1B	2A	2B	3A	3B
u		GF	SOI	GF	SOI	GF	SOI
u_{min}	[-]/[°bTDC]	0.30	35	0.30	6	0.30	8
u_{max}	[-]/[°bTDC]	0.92	49	0.92	23	0.85	20
KI_{lim}	MAPO [bar]	5.5	5.5	7	7	18	18
p	[-]	0.030	0.030	0.030	0.030	0.030	0.030
k_{ret}	[-]/[CAD]	-0.03	1	-0.03	1	-0.03	1
$p_{ki,median}$	[-]	0.030	0.053	0.030	0.032	0.032	0.028
$p_{ki,min}$	[-]	0.028	0.028	0.028	0.028	0.005	0.027
$p_{ki,max}$	[-]	0.032	0.145	0.032	0.032	0.033	0.030

It is important to note that the objective of the following validation is to evaluate the potential of the chosen variables to maintain the combustion operation to its limit by means of a knock-like controller in all the combustion modes. Hence, the KI limitation was defined according to each combustion conditions, i.e. the limit was set empirically and relatively close to the original levels, hence restricting the controller amplitude range of actuation. The definition of a global index limitation for the whole engine map was not evaluated in this work and it is therefore important to highlight that the obtained results correspond, in some extent, to a narrow range of control actuation where a more restrictive knock index limitation definition might cause control restrictions and exhibit distinct outcomes. Nevertheless, this situation is to be expected if such control strategy is activated in circumstances where the operating conditions are reaching the engine limitation and thus would ensure to not overcome it. The control implementation for activation and deactivation as a function of the combustion operation, e.g. enabled only when harmful conditions are met until safer ones are expected, was not considered here.

Each control variable, i.e. GF and SOI, was constrained as stated by the values u_{min} and u_{max} in Table 3. According to the previous combustion sensitivity analysis, it was found that the resonance level should be controlled by the gasoline fraction in fully and highly premixed conditions where a higher quantity results in lower resonance levels. The controller will therefore first attempt to reduce the gasoline fraction until a cycle is detected to overcome the limit. Even though the knock index should be detected above the limit before reaching really low GF levels, the lower limitation was set in every case to avoid pure diesel operation. Meanwhile, the upper value was set to avoid high gasoline concentration which could lead to misfire conditions and result in unstable combustion. In fully and highly premixed combustion modes, the injection timing upper limit was set to avoid injections merging with the pilot injection (i.e. dwell time limitation) while in fully premixed case the value was chosen to leave some margin to the controller action to ensure a proper evaluation in these conditions and avoid combustion regime modification. The lower injection timing limitation was chosen to avoid combustion regime transition (OP 1 and 2) or unstable operation and poor combustion efficiency (OP 3).

Figure 11 to Figure 13 show the controller behavior in three selected cases from Table 3. In each of these figures, the area in white represents the phase of the test where the controller is enabled, while when it is not, the area is colored in grey. The top plot shows the cycle-to-cycle knock index level at each cylinder, the middle plot the control actions and the bottom plot the evolution of the probability of exceeding cycles in a moving buffer of 100 cycles. The continuous black line in the top plot represents the KI limit, and the desired probability threshold in the bottom plot.

As suggested in Figure 9 and confirmed in the results in Table 3, in fully premixed operation, only the gasoline fraction is able to drive the index to the desired threshold (Test 1A), compared to the injection timing which results in an out of range probability ($p_{ki,median} = 0.053$) with high cylinder-to-cylinder probability dispersion, from a minimum of 0.028 in cylinder 3 to a maximum of 0.145 in cylinder 4 (Test 1B). Figure 11 illustrates the controller response to the conditions in Test 1A. It can be observed that the controller was able to maintain the cycles exceeding the MAPO limit to the desired probability threshold using the gasoline fraction as the control variable in all the cylinders. Once a cycle was detected above the MAPO limit (specified in Table 3), the gasoline fraction was reduced by an amount k_{ret} and slowly drove back to the limit operation. Note that in order to appreciate the final magnitude in the probability evolution, the bottom plot is cropped and some cylinders are therefore not fully represented. It is also observed that not all the cylinders have a starting probability of cycles exceeding the limit above the specified threshold (i.e. when the controller is not enabled), which shows that, if applied in a complete control strategy scenario, each cylinder might be individually enabled or not according to their original resonance levels.

Similarly to the fully premixed case, the gasoline fraction was able to maintain the combustion at its operation limit in the highly premixed case (Test 2A). On the contrary, the injection timing effect in Test 2B was less straightforward in these conditions. Figure 12 shows the results obtained when the SOI was used to control MAPO in OP 2. It is observed that the injection timing at each cylinder is individually controlled within u_{min} and u_{max} range (represented by black dashed lines) to drive the probability of the cycles exceeding the limit value towards the desired probability
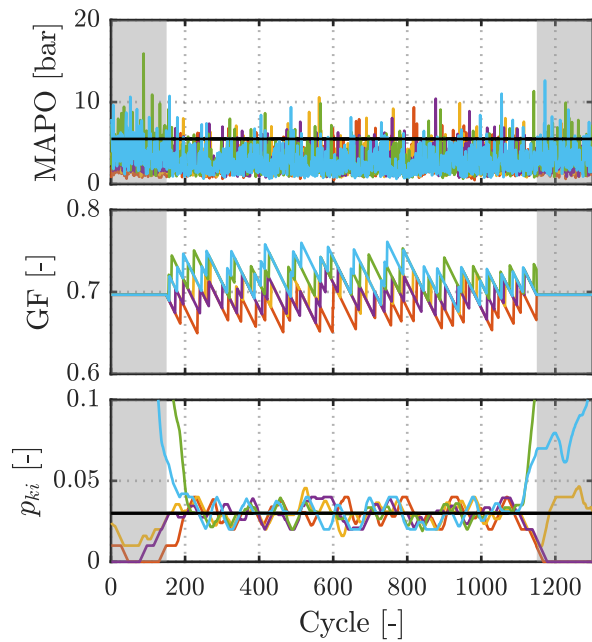
Figure 11. Test 1A, MAPO control using the gasoline fraction in fully premixed conditions (the reader is referred to Figure 6 for the cylinder color legend description). Continuous black line: MAPO limitation (top) and probability threshold (bottom)

Figure 12. Test 2B, MAPO control using the start of the main injection in highly premixed conditions (the reader is referred to Figure 6 for the cylinder color legend description). Continuous black line: MAPO limitation (top) and probability threshold (bottom), dashed black lines: control actions limitations

threshold as shown in the bottom plot. Overall, the control actions in this case show some authority but are less explicit compared to the gasoline fraction, which agrees with Figure 9 and might be explained by the in-between situation of the injection timing effect under these conditions (transition between kinetically and mixing controlled combustion).

Finally, Test 3A and Test 3B were performed to evaluate the ability of the gasoline fraction and the injection timing to control the MAPO distribution in partially premixed conditions, respectively. In Test 3A the gasoline fraction was found to not be able to control the combustion to the desired operation limit in all the cylinders as indicated in Table 3. This was expected according to the very low sensitivity found in the previous section (see Figure 9). Meanwhile, the injection timing was capable of moving and maintain the MAPO probability towards the defined threshold as shown in Figure 13. In this case the injection timing is advanced in almost all the cylinders because the starting MAPO levels were below the defined limitation.

In order to evaluate if the proposed control architecture could be applied with more traditional combustion limitation indexes, the same analysis was performed using the MPRR and the RI. The results are summarized and compared in Appendix I.

Summary and conclusion

This work studied the combustion pressure oscillations in a dual-fuel heavy-duty engine with different combustion strategies: fully, highly and partially premixed. It was observed that, although having the same load, each combustion mode presents a distinct pressure oscillations
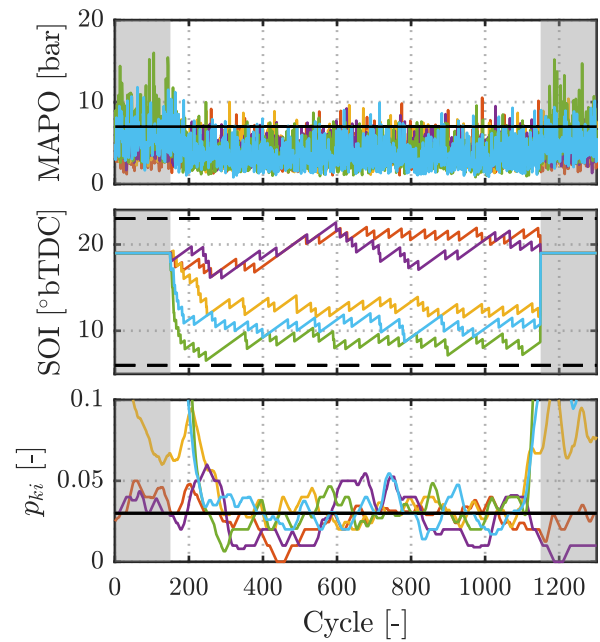

Figure 13. Test 3B, MAPO control using the start of the main injection in partially premixed conditions (the reader is referred to Figure 6 for the cylinder color legend description). Continuous black line: MAPO limitation (top) and probability threshold (bottom), dashed black line: control actions limitation
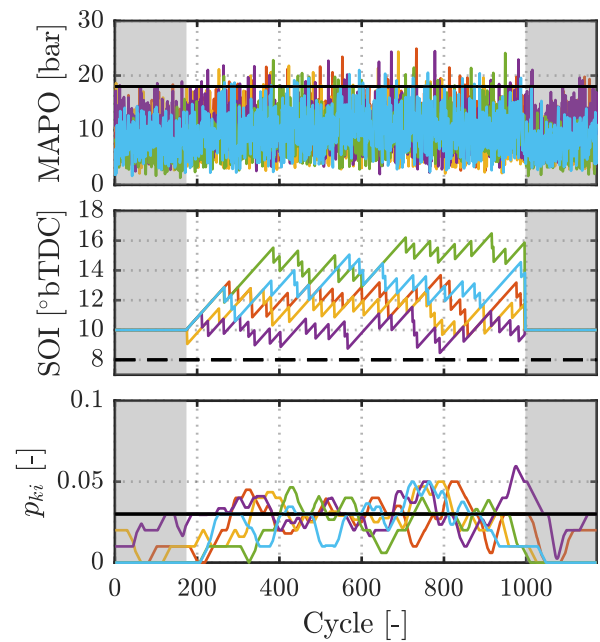
content. Three indexes were analyzed to evaluate the harmful potential of the combustion operation: the maximum pressure rise rate, the ringing intensity and the maximum amplitude of pressure oscillations. An opposite detection trend between them was found against different levels of

mixture stratification showing that common limitation based on MPRR alone does not tackle the harmful potential of the pressure oscillations.

The MAPO was chosen to represent the resonance intensity in the combustion chamber and a combustion sensitivity was performed to evaluate the potential control variables to manage its distribution at each combustion mode. The gasoline fraction and the main injection timing were explored and selected to be implemented in the control strategy.

The control application was based on the conventional knock controller in SI engines substituting the spark advance by the gasoline fraction and the injection timing. The results showed that in fully premixed conditions the controller was able to limit the pressure oscillations by regulating the mixture reactivity with the gasoline fraction. Similarly, the highly premixed condition was found to be efficiently controlled by the gasoline fraction, and the injection timing exhibited some authority to control the resulting probability in a certain proportion as well. At last, the probability of cycles exceeding the predefined limit in the partially premixed strategy was well regulated by the injection timing.

In this work, the proposed method offers a solution to control the resonance excitation intensity in premixed dual-fuel engines based on the acquisition of the in-cylinder pressure signal. Nevertheless, one could define another knock index using a conventional knock sensor placed on the engine structure instead and apply the same control strategy definition to improve the pressure oscillations limitation.

Acknowledgments

References

1. Desantes J, Benajes J, Molina S et al. The modification of the fuel injection rate in heavy-duty diesel engines. Part 1: Effects on engine performance and emissions. *Applied Thermal Engineering* 2004; 24(17-18): 2701–2714. DOI: 10.1016/j.applthermaleng.2004.05.003.
2. Asad U, Zheng M, Han X et al. Fuel Injection Strategies to Improve Emissions and Efficiency of High Compression Ratio Diesel Engines. *SAE International Journal of Engines* 2008; 1(1): 2008–01–2472. DOI:10.4271/2008-01-2472.
3. Lu X, Han D and Huang Z. Fuel design and management for the control of advanced compression-ignition combustion modes. *Progress in Energy and Combustion Science* 2011; 37(6): 741–783. DOI:10.1016/j.pecs.2011.03.003.
4. Hunicz J, Mikulski M, Geca MS et al. An applicable approach to mitigate pressure rise rate in an HCCI engine with negative valve overlap. *Applied Energy* 2020; 257(October 2019): 114018. DOI:10.1016/j.apenergy.2019.114018.
5. Kassa M, Leroy T, Robert A et al. Analysis of in-cylinder pressure oscillation and its effect on wall heat transfer. *International Journal of Engine Research* 2020; : 146808742093236DOI:10.1177/1468087420932364.
6. Nates R and Yates ADB. Knock Damage Mechanisms in Spark-Ignition Engines. In *SAE Technical Papers*. 412. DOI: 10.4271/942064.
7. Naber J, Blough JR, Frankowski D et al. Analysis of Combustion Knock Metrics in Spark-Ignition Engines. In *SAE Technical Papers*, volume 2006. DOI:10.4271/2006-01-0400.
8. Vulli S, Dunne J, Potenza R et al. Time-frequency analysis of single-point engine-block vibration measurements for multiple excitation-event identification. *Journal of Sound and Vibration* 2009; 321(3-5): 1129–1143. DOI:10.1016/j.jsv.2008.10.011.
9. Millo F and Ferraro CV. Knock in S.I. Engines: A Comparison between Different Techniques for Detection and Control. In *SAE Technical Papers*. 724. DOI:10.4271/982477.
10. Galloni E. Dynamic knock detection and quantification in a spark ignition engine by means of a pressure based method. *Energy Conversion and Management* 2012; 64: 256–262. DOI: 10.1016/j.enconman.2012.05.015.
11. Willems F. Is Cylinder Pressure-Based Control Required to Meet Future HD Legislation? *IFAC-PapersOnLine* 2018; 51(31): 111–118. DOI:10.1016/j.ifacol.2018.10.021.
12. Rogers DR. *Engine Combustion: Pressure Measurement and Analysis*. SAE international Warrendale, PA, 2010. ISBN 9780768034424. DOI:10.4271/r-388.
13. Zhen X, Wang Y, Xu S et al. The engine knock analysis – An overview. *Applied Energy* 2012; 92: 628–636. DOI: 10.1016/j.apenergy.2011.11.079.
14. Bares P, Selmanaj D, Guardiola C et al. A new knock event definition for knock detection and control optimization. *Applied Thermal Engineering* 2018; 131: 80–88. DOI:10.1016/j.applthermaleng.2017.11.138.
15. Pla B, De La Morena J, Bares P et al. Knock Analysis in the Crank Angle Domain for Low-Knocking Cycles Detection. In *SAE Technical Papers*, volume 2020-April. pp. 1–11. DOI: 10.4271/2020-01-0549.
16. Li RC and Zhu GG. A real-time pressure wave model for knock prediction and control. *International Journal of Engine Research* 2019; : 146808741986916DOI:10.1177/1468087419869161.
17. Corral-Gómez L, Rubio-Gómez G, Rodriguez-Rosa D et al. A comparative analysis of knock severity in a Cooperative Fuel Research engine using binary gasoline–alcohol blends. *International Journal of Engine Research* 2020; : 146808742091668DOI:10.1177/1468087420916683.
18. Siano D, Panza MA and D'Agostino D. Knock Detection Based on MAPO Analysis, AR Model and Discrete Wavelet Transform Applied to the In-Cylinder Pressure Data: Results and Comparison. *SAE International Journal of Engines* 2014; 8(1): 2014–01–2547. DOI:10.4271/2014-01-2547.
19. Peyton Jones JC, Spelina JM and Frey J. Optimizing knock thresholds for improved knock control. *International Journal of Engine Research* 2014; 15(1): 123–132. DOI:10.1177/1468087413482321.
20. Zhang Y, Shen X, Wu Y et al. On-board knock probability map learning–based spark advance control for combustion engines. *International Journal of Engine Research* 2019; 20(10): 1073–1088. DOI:10.1177/1468087419858026.

21. Pla B, Bares P, Jiménez I et al. A fuzzy logic map-based knock control for spark ignition engines. *Applied Energy* 2020; 280(May): 116036. DOI:10.1016/j.apenergy.2020.116036.

22. Wang Z, Liu H and Reitz RD. Knocking combustion in spark-ignition engines. *Progress in Energy and Combustion Science* 2017; 61: 78–112. DOI:10.1016/j.pecs.2017.03.004.

23. Ren Y, Randall RB and Milton BE. Influence of the resonant frequency on the control of knock in diesel engines. *Proceedings of the Institution of Mechanical Engineers, Part D: Journal of Automobile Engineering* 1999; 213(2): 127–133. DOI:10.1243/0954407991526748.

24. Torregrosa AJ, Broatch A, Margot X et al. Understanding the unsteady pressure field inside combustion chambers of compression-ignited engines using a computational fluid dynamics approach. *International Journal of Engine Research* 2020; 21(8): 1273–1285. DOI:10.1177/1468087418803030.

25. Rusly AM, Kook S, Hawkes ER et al. Effect of Pilot Injection on Diesel Knock in a Small-Bore Optical Engine. In *ASME 2012 Internal Combustion Engine Division Spring Technical Conference*. American Society of Mechanical Engineers. ISBN 978-0-7918-4466-3, pp. 225–237. DOI:10.1115/ICES2012-81023.

26. Zhang Q, Hao Z, Zheng X et al. Characteristics and effect factors of pressure oscillation in multi-injection DI diesel engine at high-load conditions. *Applied Energy* 2017; 195: 52–66. DOI:10.1016/j.apenergy.2017.03.048.

27. Jain A, Krishnasamy A and V P. Computational optimization of reactivity controlled compression ignition combustion to achieve high efficiency and clean combustion. *International Journal of Engine Research* 2020; (x): 146808742093173. DOI:10.1177/1468087420931730.

28. Jafari B, Seddiq M and Mirsalim SM. Assessment of the impacts of combustion chamber bowl geometry and injection timing on a reactivity controlled compression ignition engine at low and high load conditions. *International Journal of Engine Research* 2020; : 146808742096121DOI:10.1177/1468087420961211.

29. Paykani A, Garcia A, Shahbakhti M et al. Reactivity controlled compression ignition engine: Pathways towards commercial viability. *Applied Energy* 2021; 282(PA): 116174. DOI:10.1016/j.apenergy.2020.116174.

30. Yao M, Zheng Z and Liu H. Progress and recent trends in homogeneous charge compression ignition (HCCI) engines. *Progress in Energy and Combustion Science* 2009; 35(5): 398–437. DOI:10.1016/j.pecs.2009.05.001.

31. Asad U, Divekar P, Zheng M et al. Low Temperature Combustion Strategies for Compression Ignition Engines: Operability limits and Challenges. *SAE Technical Paper Series* 2013; 1. DOI:10.4271/2013-01-0283.

32. Paykani A, Kakaee AH, Rahnama P et al. Progress and recent trends in reactivity-controlled compression ignition engines. *International Journal of Engine Research* 2016; 17(5): 481–524. DOI:10.1177/1468087415593013.

33. Guardiola C, Pla B, Bares P et al. An analysis of the in-cylinder pressure resonance excitation in internal combustion engines. *Applied Energy* 2018; 228(March): 1272–1279. DOI:10.1016/j.apenergy.2018.06.157.

34. Eng JA. Characterization of Pressure Waves in HCCI Combustion. In *SAE Technical Paper Series*. 724. ISBN 0148-7191, pp. 2002–01–2859. DOI:10.4271/2002-01-2859.

35. Kokjohn SL, Hanson RM, Splitter DA et al. Fuel reactivity controlled compression ignition (RCCI): a pathway to controlled high-efficiency clean combustion. *International Journal of Engine Research* 2011; 12(3): 209–226. DOI:10.1177/1468087411401548.

36. Bahri B, Shahbakhti M, Kannan K et al. Identification of ringing operation for low temperature combustion engines. *Applied Energy* 2016; 171: 142–152. DOI:10.1016/j.apenergy.2016.03.033.

37. Shahlari AJ, Hocking C, Kurtz E et al. Comparison of Compression Ignition Engine Noise Metrics in Low-Temperature Combustion Regimes. *SAE International Journal of Engines* 2013; 6(1): 2013–01–1659. DOI:10.4271/2013-01-1659.

38. Wissink M, Wang Z, Splitter D et al. Investigation of Pressure Oscillation Modes and Audible Noise in RCCI, HCCI, and CDC. In *SAE Technical Papers*, volume 2. ISBN 2013011652. DOI:10.4271/2013-01-1652.

39. Dernotte J, Dec JE and Ji C. Investigation of the Sources of Combustion Noise in HCCI Engines. *SAE International Journal of Engines* 2014; 7(2): 2014–01–1272. DOI:10.4271/2014-01-1272.

40. Selim MYE. Combustion Noise Measurements and Control from Small Diesel and Dual Fuel Engines. In *SAE Technical Papers*, volume 2004-Septe. DOI:10.4271/2004-32-0072.

41. Kirsten M, Pirker G, Redtenbacher C et al. Advanced Knock Detection for Diesel/Natural Gas Engine Operation. *SAE International Journal of Engines* 2016; 9(3): 2016–01–0785. DOI:10.4271/2016-01-0785.

42. Lounici M, Benbellil M, Loubar K et al. Knock characterization and development of a new knock indicator for dual-fuel engines. *Energy* 2017; 141: 2351–2361. DOI:10.1016/j.energy.2017.11.138.

43. Chen L, Zhang R, Pan J et al. Optical study on autoignition and knocking characteristics of dual-fuel engine under CI vs SI combustion modes. *Fuel* 2020; 266(November 2019): 117107. DOI:10.1016/j.fuel.2020.117107.

44. Sjöberg M and Dec JE. Effects of Engine Speed, Fueling Rate, and Combustion Phasing on the Thermal Stratification Required to Limit HCCI Knocking Intensity. In *SAE Technical Papers*. DOI:10.4271/2005-01-2125.

45. Broatch A, Margot X, Novella R et al. Combustion noise analysis of partially premixed combustion concept using gasoline fuel in a 2-stroke engine. *Energy* 2016; 107: 612–624. DOI:10.1016/j.energy.2016.04.045.

46. Wang Y, Guo C, Wang P et al. Numerical Investigation on Knock Combustion in a Diesel–Dimethyl Ether Dual-Fuel Engine. *Energy & Fuels* 2019; 33(6): 5710–5718. DOI:10.1021/acs.energyfuels.9b00695.

47. Ott T, Zurbriggen F, Onder C et al. *Cylinder individual feedback control of combustion in a dual fuel engine*, volume 7. IFAC, 2013. ISBN 9783902823434. DOI:10.3182/20130904-4-JP-2042.00080.

48. Ingesson G, Yin L, Johansson R et al. A Double-Injection Control Strategy For Partially Premixed Combustion. *IFAC-PapersOnLine* 2016; 49(11): 353–360. DOI:10.1016/j.ifacol.2016.08.053.

49. Haskara I and Wang YY. Closed-Loop Combustion Noise Limit Control for Modern Diesel Combustion Modes. *IEEE Transactions on Control Systems Technology* 2017; 25(4): 1168–1179. DOI:10.1109/TCST.2016.2597747.

50. Guardiola C, Pla B, Bares P et al. Closed-loop control of a dual-fuel engine working with different combustion modes using in-cylinder pressure feedback. *International Journal of Engine Research* 2019; DOI:10.1177/1468087419835327.

51. Mashkournia M, Audet A and Koch CR. Knock Detection and Control in an HCCI Engine Using DWT. In *ASME 2011 Internal Combustion Engine Division Fall Technical Conference*. ASMEDC. ISBN 978-0-7918-4442-7, pp. 391–399. DOI:10.1115/ICEF2011-60076.

52. Sellnau MC, Matekunas FA, Battiston PA et al. Cylinder-Pressure-Based Engine Control Using Pressure-Ratio-Management and Low-Cost Non-Intrusive Cylinder Pressure Sensors. In *SAE Technical Papers*. 724. DOI: 10.4271/2000-01-0932.

53. Malaczynski G, Roth G and Johnson D. Ion-Sense-Based Real-Time Combustion Sensing for Closed Loop Engine Control. *SAE International Journal of Engines* 2013; 6(1): 2013–01–0354. DOI:10.4271/2013-01-0354.

54. Ängeby J, Johnsson A and Hellström K. Knock Detection Using Multiple Indicators and a Classification Approach. *IFAC-PapersOnLine* 2018; 51(31): 297–302. DOI:10.1016/j.ifacol.2018.10.063.

55. Ravaglioli V, Carra F, Moro D et al. Remote Sensing Methodology for the Closed-Loop Control of RCCI Dual Fuel Combustion. In *SAE Technical Papers*, volume 2018-April. pp. 1–10. DOI:10.4271/2018-01-0253.

56. Brunt MFJ and Pond CR. Evaluation of Techniques for Absolute Cylinder Pressure Correction. *SAE Technical Paper* 1997; (412). DOI:10.4271/970036.

57. Draper C. The physical effects of detonation in a closed cylindrical chamber. *NACA Report* 1935; (493).

58. Indrajuana A, Bekdemir C, Feru E et al. Towards Model-Based Control of RCCI-CDF Mode-Switching in Dual Fuel Engines. In *SAE Technical Paper*. ISBN 2018010263, pp. 1–13. DOI: 10.4271/2018-01-0263.

59. Benajes J, García A, Monsalve-Serrano J et al. Clean and efficient dual-fuel combustion using OMEx as high reactivity fuel: Comparison to diesel-gasoline calibration. *Energy Conversion and Management* 2020; 216(March): 112953. DOI:10.1016/j.enconman.2020.112953.

60. Kyrtatos P, Brückner C and Boulouchos K. Cycle-to-cycle variations in diesel engines. *Applied Energy* 2016; 171: 120–132. DOI:10.1016/j.apenergy.2016.03.015.

61. Payri F, Lujan J, Climent H et al. Effects of the Intake Charge Distribution in HSDI Engines. *SAE Technical Paper Series* 2010; 1. DOI:10.4271/2010-01-1119.

62. Kassa M, Hall C, Ickes A et al. Modeling and control of fuel distribution in a dual-fuel internal combustion engine leveraging late intake valve closings. *International Journal of Engine Research* 2017; 18(8): 797–809. DOI:10.1177/1468087416674426.

63. Robert A, Truffin K, Iafrate N et al. Large-eddy simulation analysis of knock in a direct injection spark ignition engine. *International Journal of Engine Research* 2019; 20(7): 765–776. DOI:10.1177/1468087418796323.

64. Dahl D, Andersson M and Denbratt I. The Origin of Pressure Waves in High Load HCCI Combustion: A High-Speed Video Analysis. *Combustion Science and Technology* 2011; 183(11): 1266–1281. DOI:10.1080/00102202.2011.589875.

65. Benajes J, Molina S, García A et al. Effects of direct injection timing and blending ratio on RCCI combustion with different low reactivity fuels. *Energy Conversion and Management* 2015; 99: 193–209. DOI:10.1016/j.enconman.2015.04.046.

66. DelVescovo D, Kokjohn S and Reitz R. The Effects of Charge Preparation, Fuel Stratification, and Premixed Fuel Chemistry on Reactivity Controlled Compression Ignition (RCCI) Combustion. *SAE International Journal of Engines* 2017; 10(4): 2017–01–0773. DOI:10.4271/2017-01-0773.

67. Kiencke U and Nielsen L. *Automotive Control Systems: For Engine, Driveline, and Vehicle*. Berlin, Heidelberg: Springer Berlin Heidelberg, 2005. ISBN 978-3-540-23139-4. DOI: 10.1007/b137654.

68. Spelina JM, Peyton Jones JC and Frey J. Stochastic simulation and analysis of a classical knock controller. *International Journal of Engine Research* 2015; 16(3): 461–473. DOI: 10.1177/1468087414551073.

Appendix I

Resonance indexes control comparison

As the MPRR is widely used in feedback applications for combustion operation limitation, and since the RI was developed to evaluate the pressure oscillations in the cylinder without measuring them directly, it was decided to apply the control strategy described previously with such indexes and to compare the results with the ones obtained using the MAPO limitation. The conditions were equivalent to the ones presented in Table 3 at the exception that the KI_{lim} were modified according to the considered index and combustion mode as indicated in Table 4.

Figure 14 shows the results for each index in all the tests in a similar way than indicated in Table 3: the median probability $p_{ki,median}$ for cylinders 2 to 6 is illustrated in a circle (GF actuation) or diamond shape (SOI actuation) and the extreme probabilities ($p_{ki,min}$ and $p_{ki,max}$) are shown with errorbars. Comparable results were observed in fully premixed conditions (Test 1A and 1B): the gasoline fraction was able to maintain the probability of exceeding cycles at the specified threshold for every index, while the injection timing resulted in high cylinder-to-cylinder dispersion with probabilities distant from the desired value. Same conclusions than with the MAPO behavior can be drawn when using MPRR and RI in Test 2A, 2B and 3B, while a greater responsiveness to the gasoline fraction was found in the partially premixed mode in Test 3A. Indeed, in this combustion mode both MPRR and RI exhibited some sensitivity as it is illustrated in Figure 15. In this figure, which compares the distribution of the three indexes in the same cylinder against control variables variations in all the combustion modes, it can be seen that unlike the MAPO, an increase in the gasoline fraction resulted in a, although slight, decrease in the MPRR and the RI in OP 3. In this case, the mixture reactivity sweep was sufficient to cause a change in the combustion evolution measured with the low-pass filtered pressure trace where the pressure rise rate and the ringing intensity are obtained from, but was not sufficient to appreciate an important change in the resonance excitation in the combustion chamber. Furthermore, it can be highlighted that in partially premixed conditions the MAPO distribution exhibits high levels with a high cycle-to-cycle

Table 4. Knock index limitations for MPRR and RI

		OP 1		OP 2		OP 3	
	Test	1A	1B	2A	2B	3A	3B
u		GF	SOI	GF	SOI	GF	SOI
KI_{lim}	MPRR [bar/CAD]	9	9	7	7	8	8
	RI [MW/m^2]	7.5	7.5	4.5	4.5	5.5	5.5

variation, representative of the stochastic nature of this index, which therefore might results in a more challenging case to ensure authority over the probability of exceeding cycles.
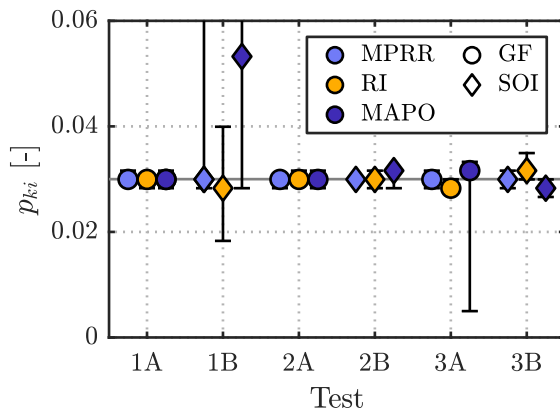

Figure 14. Probability results of KI occurrences above the desired limit. The continuous grey line shows the desired probability threshold ($p = 0.03$)

This analysis shows that although indexes based on the direct measurement of the pressure oscillations would be of greater interest to limit their intensity by means of stochastic control, more traditional indexes such as the MPRR or the RI might also be used in the same control architecture and be able to limit the combustion operation, as long as a sensitivity to the control variables is evidenced.
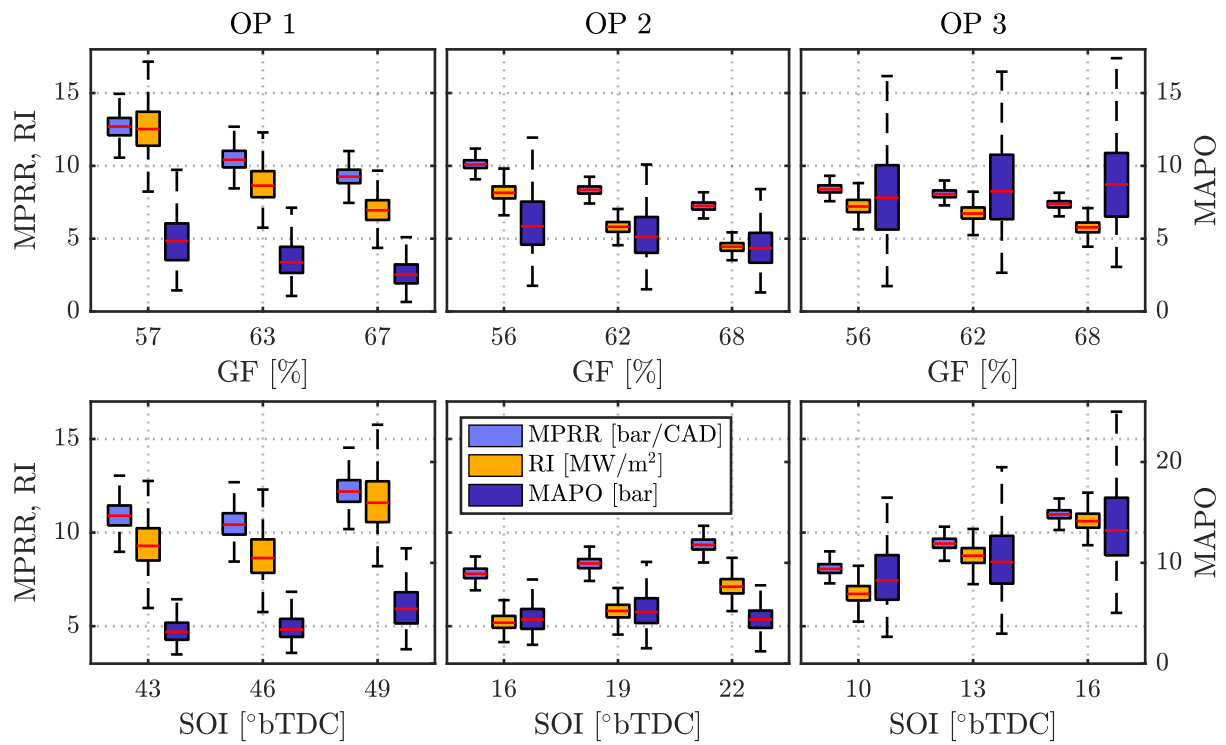
Figure 15. Combustion sensitivity to control inputs in all the dual-fuel combustion modes for all the indexes: gasoline fraction (top plots) and diesel injection timing (bottom plots)